Science Journal of Energy Engineering
2026, Vol. 14, No. 3, pp. 83–97
https://doi.org/10.11648/j.sjee.20261403.12

Research Article

Assessment of the Impact of Climatic Variations on the Photovoltaic Potential of Kankan (Guinea) Using NASA POWER Data and Artificial Neural Network (2000–2025)

Papa Lat Tabara Sow[1], Mamadou Traore[1, 2, 3, *], Daouda Gueye[3], Amadou Sidibe[2], Amadou Ba[3], Cheikh Saliou Toure[1, 4], Vone Beavogui[2], Alphousseyni Ndiaye[3], Senghane Mbodji[1], Faoro Eugene Maomou[2]

[1]Materials and Laser of Department of Physics, Alioune Diop University of Bambey, Bambey, Senegal
[2]Departement of Physics, University of Julius Nyerere of Kankan, Kankan, Guinea
[3]Efficiency and Energetic System of Department of Physics, Alioune Diop University of Bambey, Bambey, Senegal
[4]Department of Photovoltaic Energy, University of Labe, Labe, Guinea

Abstract

West Africa benefits from strong solar resources, yet in Guinea the influence of climate change on photovoltaic availability has received little attention. This work evaluates the effects of climate change on the photovoltaic potential of Kankan (Guinea) using daily data from the NASA POWER database for 2000-2025. The study focuses on global solar irradiation, air temperature, relative humidity, and wind speed. A semi-empirical model is used to estimate daily photovoltaic potential, and trends are analyzed with linear regression and the non-parametric Mann-Kendall test. In parallel, a multilayer perceptron artificial neural network (MPANN) is developed to reproduce the estimated photovoltaic potential from the selected climatic inputs. The analysis shows significant declines in air temperature (-0.0559 ℃ year^{-1}) and wind speed (-0.0077 ms^{-1}year^{-1}), together with a significant rise in relative humidity (+0.6249% year^{-1}). Global solar irradiation presents no statistically significant trend over the study period. Despite these changes, the photovoltaic potential remains broadly stable, with a small and statistically non-significant decrease of -0.0152 kWh day^{-1}year^{-1} ($p = 0.186 > 0.05$). The MPANN delivers very high predictive performance, with the coefficient of determination of 0.99, the mean absolute error (MAE) of 0.0266 kWh day^{-1}, the root mean square error (RMSE) of 0.0478 kWh day^{-1}, and the mean absolute percentage error (MAPE) of 0.134%. Overall, the climatic shifts observed in Kankan during the last twenty-six years have not significantly altered the region’s photovoltaic potential. This stability supports the suitability of solar energy as a sustainable option to meet Guinea’s growing energy needs. The study also highlights the usefulness of artificial intelligence methods for assessing and forecasting renewable energy resources in tropical regions.

Keywords

Climate Variability, Photovoltaic Potential, Artificial Neural Network, NASA POWER, Mann–Kendall Test, Kankan, Guinea

*Correspondence: Mamadou Traore (mamadoutraore1uadb@gmail.com)

Received: 25 August 2026; **Accepted:** 7 September 2026; **Published:** 24 September 2026

1. Introduction

Rising global energy use, growing concern over climate change, and the gradual exhaustion of fossil fuels are speeding up the transition to more sustainable energy systems [1, 2]. Because the energy sector is a major source of anthropogenic greenhouse gas emissions, scaling up renewables is essential to cut emissions while keeping pace with increasing demand [1, 3, 4]. Among low-carbon technologies, solar photovoltaics has expanded the most rapidly worldwide, with installed capacity exceeding 1,400 GW in 2023, a surge supported by sharp declines in manufacturing costs and steady gains in module efficiency [5-7]. Sub-Saharan Africa, which benefits from some of the strongest solar resources on the planet, has clear opportunities to extend electricity access, enhance energy security, and foster socio-economic development [7, 8]. However, PV output is highly sensitive to local weather. Air temperature determines cell operating temperature, and higher values generally reduce conversion efficiency [9]. Relative humidity affects the amount of radiation reaching the modules and thus their output, while wind improves natural cooling and limits thermal losses [10, 11]. Climate change is expected to shift several atmospheric variables simultaneously, with implications for both the solar resource and PV efficiency [12-15]. Recent studies suggest that PV responses to climate are governed mainly by the combined influence of multiple meteorological factors rather than changes in irradiance alone [16, 17]. Drawing on CORDEX-Africa simulations, Bichet et al. concluded that the continent is likely to preserve strong photovoltaic potential despite future climate change [18]. In a similar direction, Danso et al. [19] and Agbor et al. [20] reported spatial differences in solar radiation and PV power production across West Africa under various climate scenarios. Despite these contributions, notable gaps persist. First, many studies prioritize changes in solar irradiance without jointly examining other climatic variables such as air temperature, relative humidity, and wind speed, even though these parameters have significant effects on PV performance [21, 22]. Second, although artificial intelligence has demonstrated strong capabilities for PV modeling and forecasting, its application to assessing climate change impacts on PV potential in West Africa remains limited, and predictive approaches are still at an early stage [23]. Third, Guinea has received relatively little focused research despite its considerable solar potential, and most analyses operate at regional or national scales, leaving a shortage of site-specific assessments for locations such as Kankan [24, 25]. With high annual insolation and rising electricity demand, Kankan region provides a relevant case study to advance Guinea's renewable energy efforts [26]. Moreover, daily climate data from the NASA POWER database over twenty-six years offer a solid basis for investigating recent climate patterns and evaluating their potential effects on local solar resources [27]. This study stands out by integrating a historical climate analysis, a semi-empirical model of PV potential, and artificial intelligence techniques, with particular attention to artificial neural networks [28-30]. We analyze how climate variability has affected the PV potential of Kankan from 2000 to 2025 by jointly considering global solar irradiance, air temperature, relative humidity, and wind speed, and we develop a neural network that reproduces PV potential derived from these climatic drivers.

2. Materials and Methods

This section presents the study area, climate dataset, data pre-processing procedure, photovoltaic potential modelling, statistical methods used for trend analysis, development of the artificial neural network and the metrics for performance adopted to evaluate the predictive model.

2.1. Study Area

In eastern Guinea's Upper Guinea region, the study site was the city of Kankan (Figure 1). Its location is near 10.38 °N and 9.30 °W, and it lies at a mean altitude of 376 m above sea level [26].

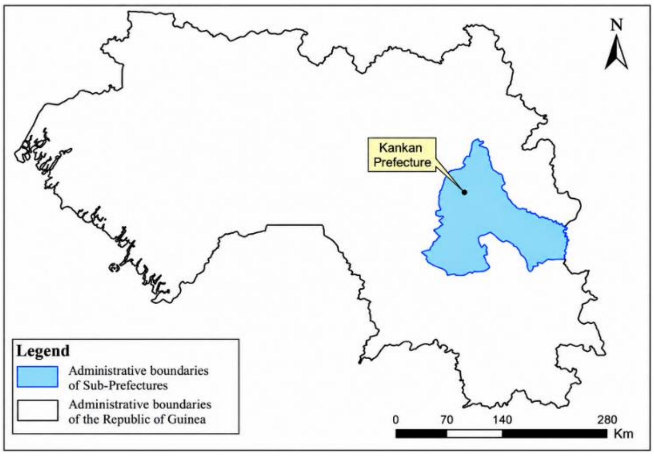

Figure 1. *Map of Kankan prefecture.*

2.2. Methodological Framework

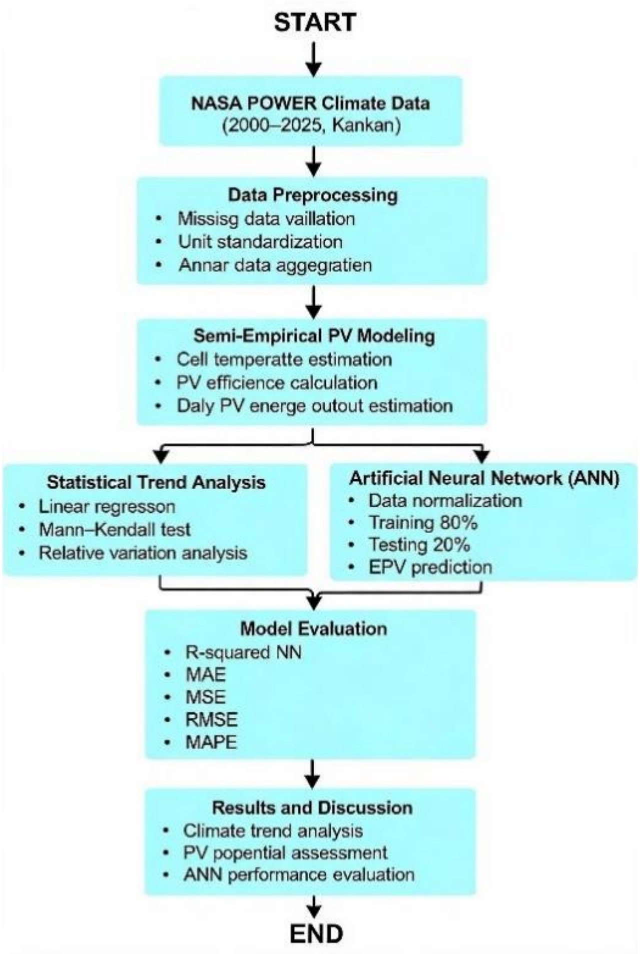

Figure 2. *Flowchart illustrating of the study.*

Figure 2 presents the methodological framework used in this study. We first preprocessed the daily climate data retrieved from the NASA POWER database to ensure data quality and temporal coherence. We then used the processed dataset to estimate photovoltaic potential with a semi-empirical model that integrates global solar irradiation, air temperature, relative humidity, and wind speed. Climatic trends were analyzed using statistical techniques, and an artificial neural network (ANN) was developed to reproduce the estimated photovoltaic potential. Finally, the ANN's performance was assessed using several statistical indicators, followed by an interpretation of the results.

2.3. Climatic Data

Climate data for this analysis were sourced from the NASA POWER platform (Prediction Of Worldwide Energy Resources) [27]. We extracted daily time series spanning 1 January 2000 to 31 December 2025. The dataset includes global solar irradiation, average air temperature, relative humidity, and wind speed recorded at 2 m above ground level.

2.4. Data Preprocessing

After downloading, the data underwent preprocessing that involved screening for missing entries, detecting outliers, and confirming the temporal consistency of the time series. To examine long-term climate patterns, we converted the daily records into annual means, a standard method that reduces the impact of seasonal variability.

2.5. Photovoltaic Potential Modeling

Photovoltaic potential is evaluated with a semi-empirical scheme (Equations (1) to (5)) that jointly accounts for global solar irradiance (G), ambient air temperature (T), relative humidity (HR), and wind speed (V). Cell temperature (T_{cell}) is derived from empirical relations validated in the literature (Equation (3)). The influence of relative humidity (K_{HR}: Equation (4)) is introduced through a correction factor informed by studies on atmospheric transmittance [9, 11, 21, 31].

$$E_{PV} = G.S.\eta_{PV}.K_{HR}.PR \tag{1}$$

Where:

$$\eta_{PV} = \eta_{ref}[1-\beta(T_{cell}-20)] \tag{2}$$

$$T_{cell} = T + \left(\frac{1000G}{24}\right)\left(\frac{NOCT-20}{800}\right) - \alpha V \tag{3}$$

$$K_{HR} = 1-0.001\left(HR-HR_{ref}\right) \tag{4}$$

$$E_{PV} = G.S.PR.\eta_{ref}.\left[1-\beta\left(T+1000G\,\frac{(NOCT-20)}{800}.24\right)-\alpha V-25\right].\left(1-\gamma\left(HR-HR_{ref}\right)\right) \tag{5}$$

Where S is the total PV panel area, η_{ref} is the reference module efficiency, η_{PV} is module efficiency, PR is the performance ratio, β is the temperature coefficient, NOCT is the nominal operating cell temperature, α is the wind cooling coefficient, γ is the humidity correction coefficient and HR_{ref} is the reference relative humidity. The numerical values of these parameters are listed in Table 1.

Table 1. *Numerical values of the parameters adopted in the semi-empirical photovoltaic model.*

Symbol	Value	Unit
S	30	m^2
η_{ref}	0.18	–
PR	0.80	–
β	0.004	℃-1
NOCT	45	℃
α	1.5	–
γ	0.001	%-1
HR_{ref}	50	%

2.6. Statistical Analysis of Climatic Trends

Examining climate trends is crucial for evaluating how climate variability affects photovoltaic potential. In this work, we apply several statistical techniques to describe the temporal evolution of global solar irradiation (G), air temperature (T), relative humidity (RH), wind speed (V), and photovoltaic potential (E_{PV}) from 2000 to 2025. The approach combines linear regression, the coefficient of determination (R^2), percentage variation, the non-parametric Mann–Kendall test [32], and Kendall's Tau coefficient. These techniques are widely used in climate and environmental research to detect and quantify trends over time [32-36]. The related formulations are presented in Equations (6)-(10).

Where:

Let $y = \{G, T, HR, E_{PV}\}$, where G, T, RH, and V correspond to global solar irradiation, air temperature, relative humidity, and wind speed, and E_{PV} denotes the photovoltaic potential. For a given year i, y_i is the observed value, $\hat{y}_i$ is the value predicted by the linear regression model, and $\overline{y}_i$ is the mean of the corresponding time series for each of these variables. The study spans n years, with n = 26.

2.6.1. Linear Regression

We applied linear regression, as specified in Equation (6), to measure the average change of the variable over time by estimating the slope of the fitted trend line. A positive slope reflects an upward trend in the variable under study, whereas a negative slope reflects a downward trend [35].

$$y(t) = at + b \tag{6}$$

2.6.2. Coefficient of Determination of the Trend (R^2_{Trend})

Following Equation (7), we used the trend's coefficient of determination to evaluate how well the fitted trend line matches the observed data. This coefficient indicates the share of the total variance accounted for by the linear regression model [21].

$$R^2_{Trend} = 1 - \frac{\sum_{i=2000}^{2025}(y_i - \hat{y}_i)^2}{\sum_{i=2000}^{2025}(y_i - \overline{y}_i)^2} \tag{7}$$

2.6.3. Percentage Variation

Equation (8) defines the percentage variation, a straightforward and useful measure of how much a variable changes from the start to the end of a period. This metric is commonly applied in climate science and photovoltaic research to quantify relative differences and to evaluate the strength of observed trends [23].

$$\Delta y(\%) = \frac{y_{2025} - y_{2000}}{y_{2000}} . 100 \tag{8}$$

2.6.4. Mann–Kendall Test

The Mann–Kendall test, described by Equation (9), is a widely used non-parametric statistical test for detecting monotonic trends in climatic, hydrological, and environmental time series. Its main advantage is that it does not require any assumption regarding the underlying distribution of the data [23, 35].

$$S_y = \sum_{i=1}^{n-1} \sum_{j=i+1}^{n} sgn(y_j - y_i) \tag{9}$$

$$sgn(y_j - y_i) = \begin{cases} 1 & if \quad y_j > y_i \\ 0 & if \quad y_j = y_i \\ -1 & if \quad y_j < y_i \end{cases}$$

2.6.5. Kendall's Tau Coefficient

The strength and direction of the trends found by the Mann–Kendall test are measured by the Kendall's Tau coefficient as shown in Equation (10). It provides an important additional index for analysing climatic and environmental time series, as it measures both the strength and the direction of the observed trends [23, 35].

$$\tau = \frac{S_y}{\frac{n(n-1)}{2}} \tag{10}$$

$$-1 \leq \tau \leq 1$$

A positive Kendall's Tau reflects an upward trend, a negative value reflects a downward trend, and a value near zero suggests no monotonic trend.

2.7. Development of an Artificial Neural Network

A multilayer perceptron (MLP) was designed to reproduce the estimated photovoltaic potential using global solar irradiation (G), air temperature (T), relative humidity (RH), and wind speed (V). The approach follows Mellit and Kalogirou [29], who showed that ANNs are effective for modeling photovoltaic systems. The dataset included 9,497 daily records. All variables were standardized with the StandardScaler and then partitioned into training and test sets in an 80%–20% split. The adopted architecture comprised four input neurons, three hidden layers with 32, 16, and 8 neurons, and a single output neuron, yielding a 4-32-16-8-1 topology. The hidden layers used the Rectified Linear Unit (ReLU) activation function, while the output layer used a linear activation suited to regression. Figure 3 presents the architecture of the implemented network. The model was trained with the Adam optimizer by minimizing the mean squared error (MSE) loss.

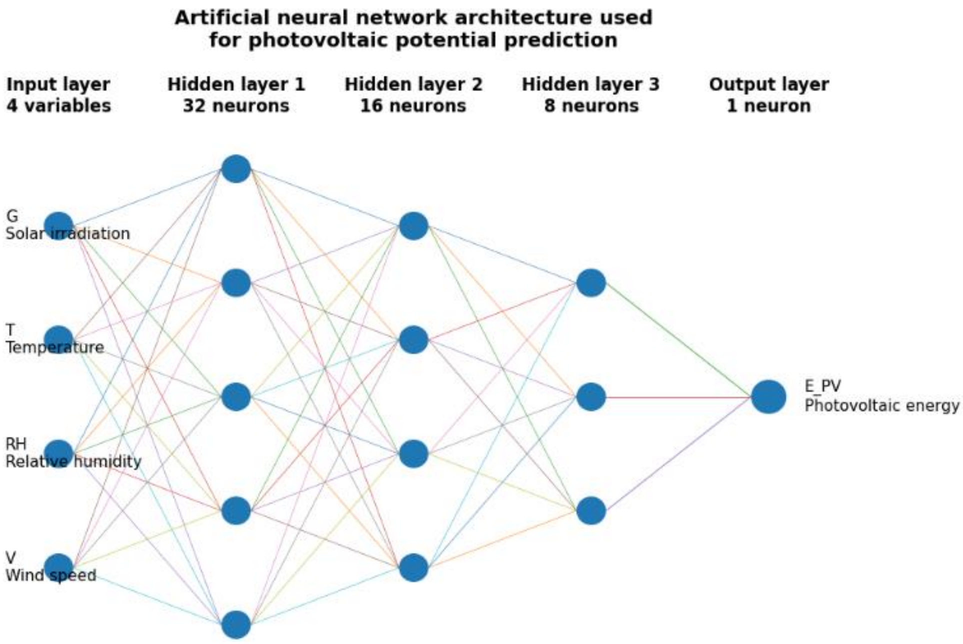

Figure 3. *Architecture of the artificial neural network.*

The ANN's performance was assessed using standard statistical indices commonly applied in energy modeling: the coefficient of determination (R^2), mean absolute error (MAE), mean squared error (MSE), root mean square error (RMSE), and mean absolute percentage error (MAPE). This choice aligns with recommendations from the National Renewable Energy Laboratory (NREL, 2020) and with established practice in the field [22, 23, 37-39]. The metrics are defined in Equations (11)-(15), where:

N denotes the number of samples in the test set; $E_{PV,i}^{cal}$ is the photovoltaic potential computed by the semi-empirical model for sample i; and $E_{PV,i}^{pre}$ is the photovoltaic potential predicted by the ANN for the same sample. The study used 9,497 daily observations, with 80% allocated to training and 20% reserved for testing.

2.7.1. Coefficient of Determination (R_{ANN}^2)

As stated in Equation (11), the coefficient of determination measures the proportion of variance in the estimated photovoltaic potential that the ANN explains. An R_{ANN}^2 value close to 1 indicates that the model delivers very strong predictive performance.

$$R_{ANN}^2 = 1 - \frac{\sum_{i=1}^{N}\left(E_{PV,i}^{cal} - E_{PV,i}^{pre}\right)^2}{\sum_{i=1}^{N}\left(E_{PV,i}^{cal} - \overline{E_{PV,i}^{pre}}\right)^2} \tag{11}$$

2.7.2. Mean Absolute Error (MAE)

According to equation (12), the mean absolute error (MAE) is the average of the absolute differences between the photovoltaic potential produced by the semi-empirical model and that predicted by the ANN. It reflects the typical size of the prediction error and uses the same unit as the photovoltaic potential.

$$MAE = \frac{1}{N}\sum_{i=1}^{N}\left|E_{PV,i}^{cal} - E_{PV,i}^{pre}\right| \quad (12)$$

2.7.3. Mean Squared Error (MSE)

Equation (13) introduces the mean squared error (MSE) as the average of the squared discrepancies between the semi-empirical estimate of photovoltaic potential and the ANN prediction.

$$MAE = \frac{1}{N}\sum_{i=1}^{N}\left(E_{PV,i}^{cal} - E_{PV,i}^{pre}\right)^2 \quad (13)$$

2.7.4. Root Mean Square Error (RMSE)

The root mean square error (RMSE), defined in Equation (14), is the square root of the MSE. It summarizes the overall prediction error of the ANN and is reported in the same unit as the photovoltaic potential (kWh day^{-1}).

$$RMSE = \sqrt{\frac{1}{N}\sum_{i=1}^{N}\left(E_{PV,i}^{cal} - E_{PV,i}^{pre}\right)^2} \quad (14)$$

2.7.5. Mean Absolute Percentage Error (MAPE)

The mean absolute percentage error (MAPE), specified in equation (15), gives the average relative difference between the semi-empirical estimate and the ANN prediction of photovoltaic potential. Expressing errors as percentages enables performance comparisons that do not depend on the magnitude of the photovoltaic potential.

$$MAPE = \frac{100}{N}\sum_{i=1}^{N}\left|\frac{E_{PV,i}^{cal} - E_{PV,i}^{pre}}{E_{PV,i}^{cal}}\right| \quad (15)$$

3. Results and Discussion

3.1. Evolution of Annual Mean of Climate Parameters

Figure 4 indicates a steady decline in the annual mean air temperature in Kankan from 2000 to 2025. The estimated annual slope of −0.0559°C year^{-1} points to a moderate downward trend, and the Mann–Kendall test shows that this trend is statistically significant ($p = 0.047 < 0.05$). The negative Kendall's Tau value (−0.28) also supports this decline (Table 2). This decrease contrasts with the global patterns reported by the IPCC, which generally describe warming at the global scale. Nevertheless, many studies have shown that local climate trends can temporarily diverge from global tendencies because of regional characteristics, rainfall variability, and local atmospheric processes [40-43]. From a photovoltaic standpoint, cooler air temperatures are advantageous. Higher photovoltaic cell temperatures typically lower module electrical efficiency. Therefore, the gradual cooling observed in Kankan is likely to reduce thermal losses and modestly improve the potential energy output of photovoltaic systems.

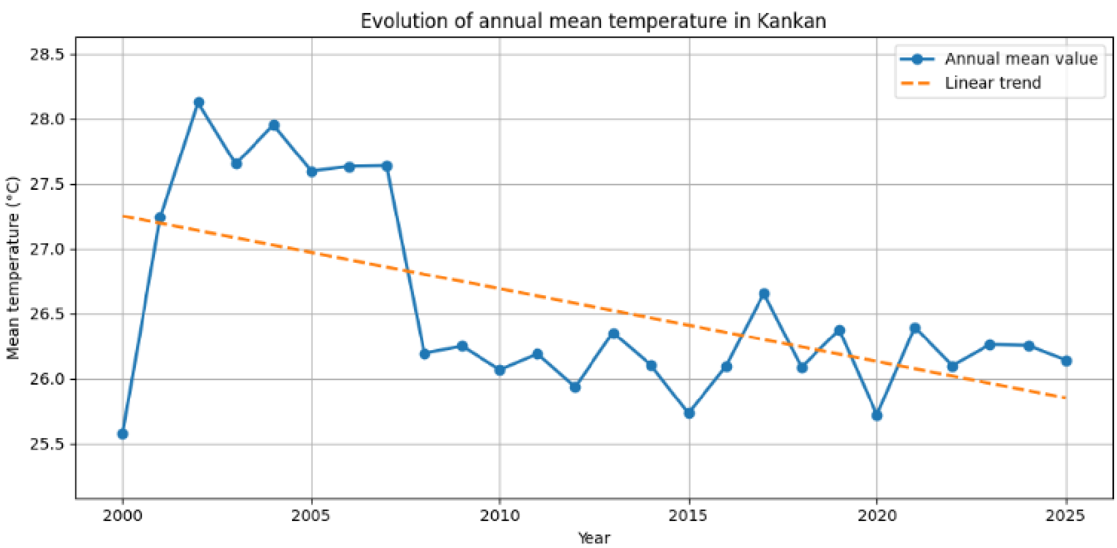

Figure 4. *Evolution of the annual mean air temperature in Kankan from 2000 to 2025, showing the fitted linear trend.*

Figure 5 shows how annual mean global solar irradiation has changed over the study period. The solar resource appears highly stable overall. The estimated linear slope is very small at -0.0012 kWh m-2day-1 per year, and the coefficient of determination for this trend is also low (R_{Trend}^2 = 0.0129), indicating no clear long-term signal (Table 2). The Mann-Kendall test supports this conclusion, with a non-significant result ($p = 0.454 > 0.05$). Although there is a modest total decline of 2.86% across the period, year-to-year variability remains fairly limited (Table 2). These results are in line with Bichet et al. [18] and Soares et al. [44], who reported that solar resources across Africa are expected to remain broadly stable despite climate change. This stability is encouraging for solar energy development in Guinea, as the solar resource has remained virtually unchanged for more than two decades.

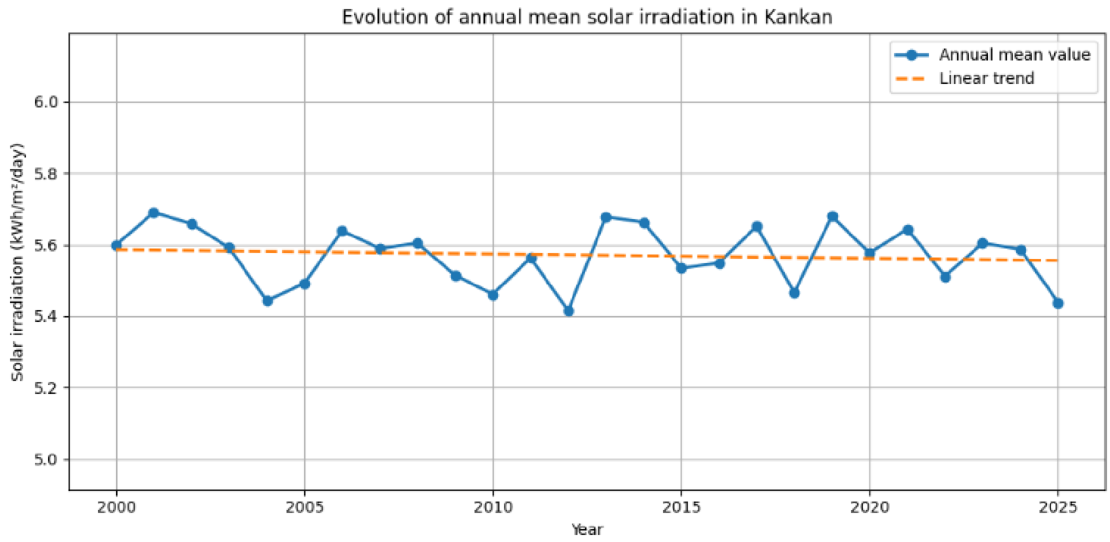

Figure 5. *Evolution of the annual mean global solar irradiation in Kankan from 2000 to 2025, showing the fitted linear trend.*

Figure 6 indicates a marked rise in the annual mean relative humidity. The linear trend shows a slope of 0.625% per year, and the associated coefficient of determination is relatively high (R^2_{Trend}= 0.5736), which means the temporal trend explains a substantial share of the observed variability (Table 2). The Mann-Kendall test independently confirms this pattern, revealing a significant upward trend ($p < 0.001$) with a Kendall's Tau of 0.5754 (Table 2). Among the climatic variables examined, relative humidity displays the most pronounced temporal signal. The increase in atmospheric moisture can alter the transfer of solar radiation through the atmosphere by amplifying scattering and absorption. Moreover, high relative humidity can accelerate certain degradation processes in photovoltaic components. Overall, the rise in relative humidity appears to be one of the principal adverse climatic factors identified in this study.

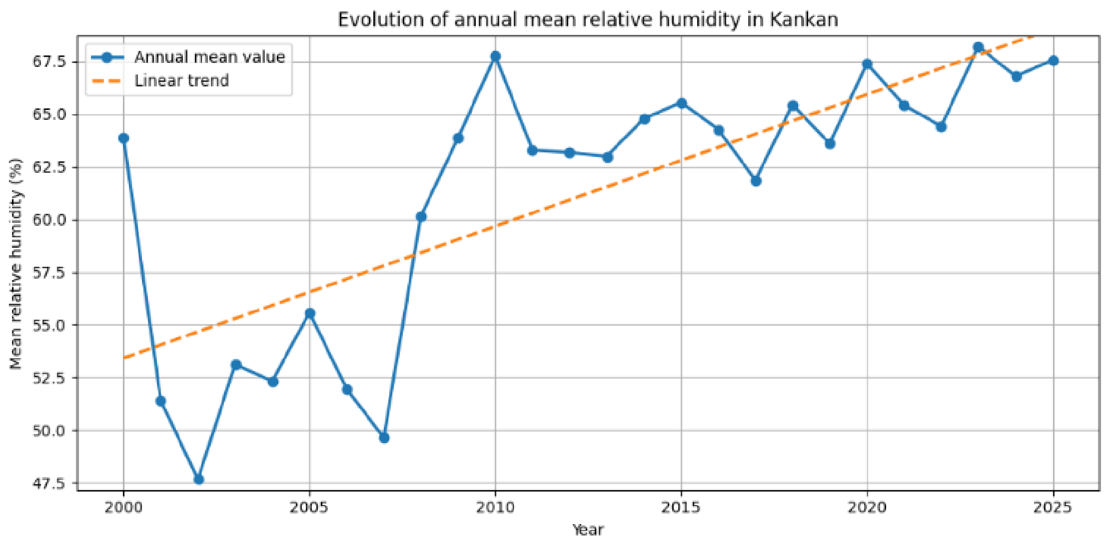

Figure 6. *Evolution of the annual mean relative humidity in Kankan from 2000 to 2025, showing the fitted linear trend.*

Figure 7 indicates a progressive decline in the yearly average wind speed. The annual trend is −0.0077 m s^{-1} per year, which is modest in magnitude but statistically significant according to the Mann–Kendall test (p = 0.017) (Table 2). This reduction matters for photovoltaic systems. Wind enhances the natural cooling of photovoltaic panels and helps limit the rise in cell temperature. As a result, lower wind speeds reduce this cooling effect. Faiman [45] and Skoplaki and Palyvos [9] showed that wind speed is a crucial factor in the thermal behavior of photovoltaic modules. Consequently, the observed decline in wind speed may slightly lower the efficiency of photovoltaic systems, even though global solar irradiation remains generally stable.

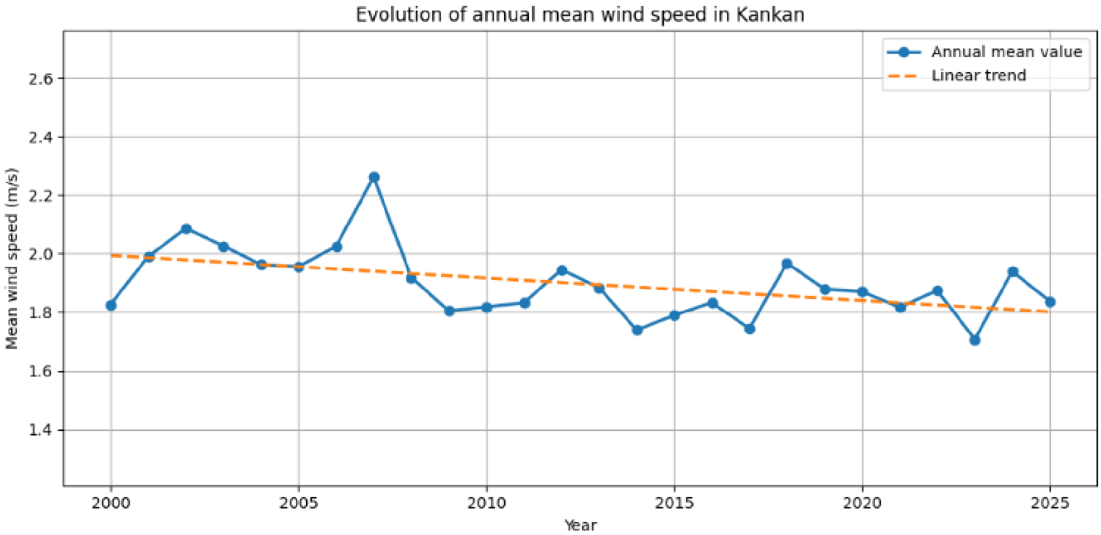

Figure 7. *Evolution of the annual mean wind speed in Kankan from 2000 to 2025, showing the fitted linear trend.*

Table 2. *Evolution of annual mean temperature, solar irradiation, relative humidity and wind speed.*

	Temperature	Solar irradiation	Relative humidity	Wind speed
Annual slope	-0.055 ℃/year	-0.001 kWh/m^2/day/year	0.624%/year	-0.008 m/s/year
Trend R^2	0.3247	0.0129	0.5736	0.238
Total variation (%)	2.197	-2.864	5.787	0.533
Mann-Kendall test	decreasing	no trend	Increasing	Decreasing
Kendall Tau	-0.28	-0.1077	0.5754	-0.335
p-value	0.0472	0.453	4.136^{-5}	0.017
Significant at 5%:	Yes	No	Yes	Yes

3.2. Evolution of Photovoltaic Potential

Figure 8 and Table 3 depict how the annual mean photovoltaic potential has changed based on the semi-empirical model developed in this study. Across the study period, a modest downward trend appears, with an estimated linear rate of −0.0152 kWh day^{-1} $year^{-1}$. However, the Mann-Kendall test shows that this trend is not statistically significant (p = 0.186 > 0.05). In line with this, the coefficient of determination for the linear fit is low (R^2_{Trend} = 0.096; see Table 3), pointing to marked interannual variability. Taken together, the results indicate that the climatic changes observed in Kankan have not led to a significant decline in photovoltaic potential. The relative stability of global solar irradiation and the decrease in air temperature partly offset the negative effects of rising relative humidity and declining wind speed.

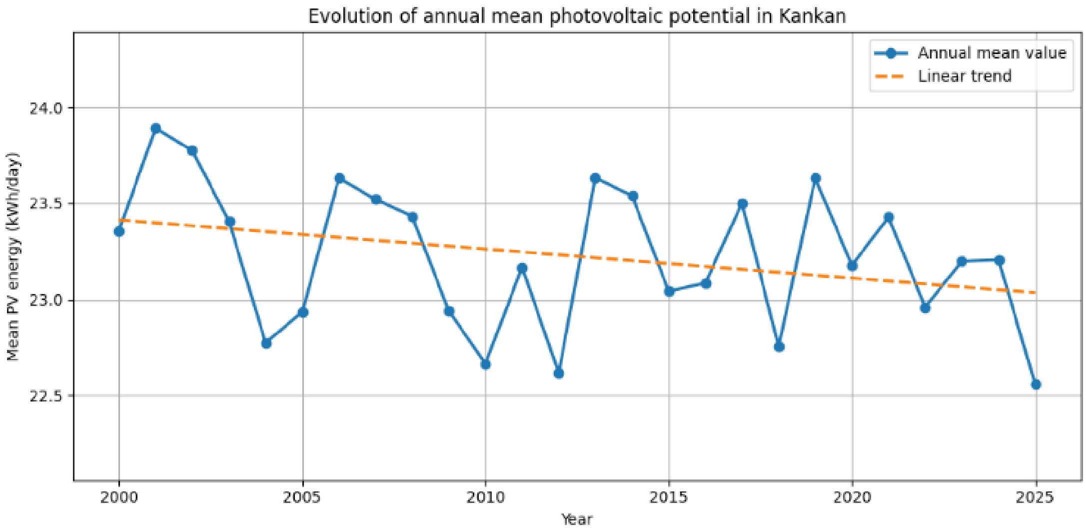

Figure 8. *Evolution of the annual photovoltaic potential in Kankan from 2000 to 2025, showing the fitted linear trend.*

Table 3. *Evolution of annual mean photovoltaic potential in Kankan.*

Annual slope	**-0.0152kWh/day/year**
R^2_{Trend}	0.096
Total variation	-3.431%
Mann-Kendall test	no trend
Kendall Tau	-0.1877
p-value	0.186
Significant at 5%:	No

3.3. Performance of the Artificial Neural Network

Table 4. *Complete ANN model evaluation.*

R^2	**0.99**
MAE	0.0266 kWh/day
MSE	0.00229
RMSE	0.0478 kWh/day
MAPE	0.134%

The performance of the developed artificial neural network (ANN) for photovoltaic potential estimation was evaluated using the statistical metrics given in Table 4. The results show an extremely high coefficient of determination (R^2_{ANN} = 0.99) which means that the model explains more than 99.98% of the variance in the estimated photovoltaic potential. The low error values, MAE of 0.0266 kWh day^{-1}, RMSE of 0.0478 kWh day^{-1} and MAPE of 0.134% are indicative of the model's strong prediction accuracy. Overall, these results show that the ANN can successfully supply the nonlinear relations between global solar irradiation, air temperature, relative humidity, wind speed and the estimated photovoltaic potential.

Figure 9 shows the time evolution of the photovoltaic potential calculated using the semi-empirical model and the values predicted by the ANN for the whole test data set. The two curves are nearly indistinguishable over the complete range of samples, indicating that the ANN replicates the variations in photovoltaic potential with very high fidelity. This visual agreement is in line with the strong values reported for the statistical performance indicators.

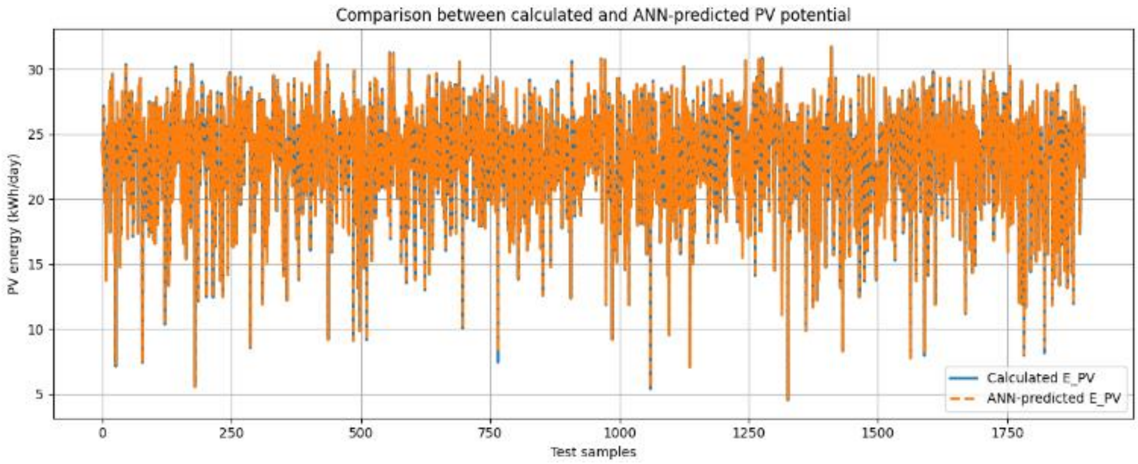

Figure 9. *Comparison between the photovoltaic potential estimated by the semi-empirical model and that predicted by the ANN model for the testing dataset.*

The correlation between the semi-empirical estimates and the ANN predictions of photovoltaic potential is presented in Fig. 10. The data points are firmly clustered along the identity line (y=x) indicating a very close correspondence between the two sets. This pattern confirms that there is no systematic bias, no consistent underestimation or overestimation by the ANN.

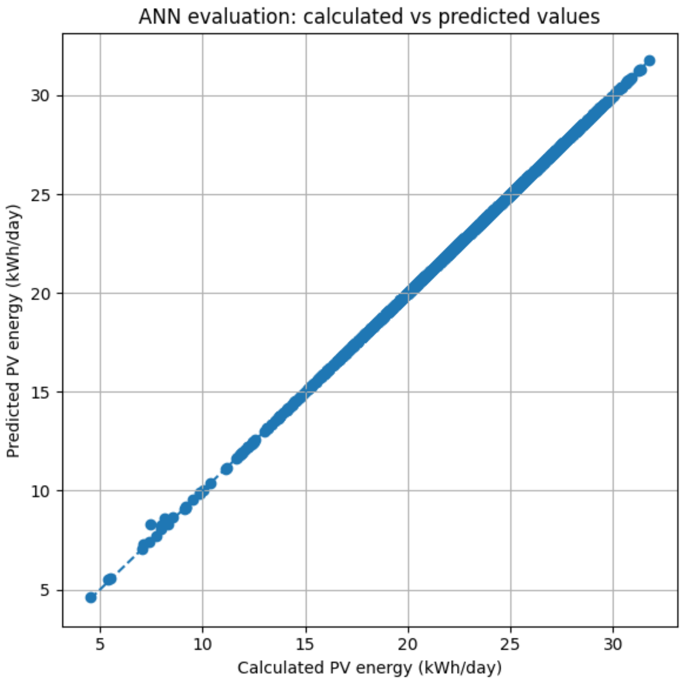

Figure 10. *Correlation between estimated and ANN-predicted photovoltaic potential.*

Figure 11 indicates that the prediction residuals are tightly clustered around zero. This pattern points to the absence of any noticeable systematic bias in the ANN outputs. The narrow dispersion of errors also supports the model's stability and its capacity to deliver accurate estimates under a wide range of climatic conditions.

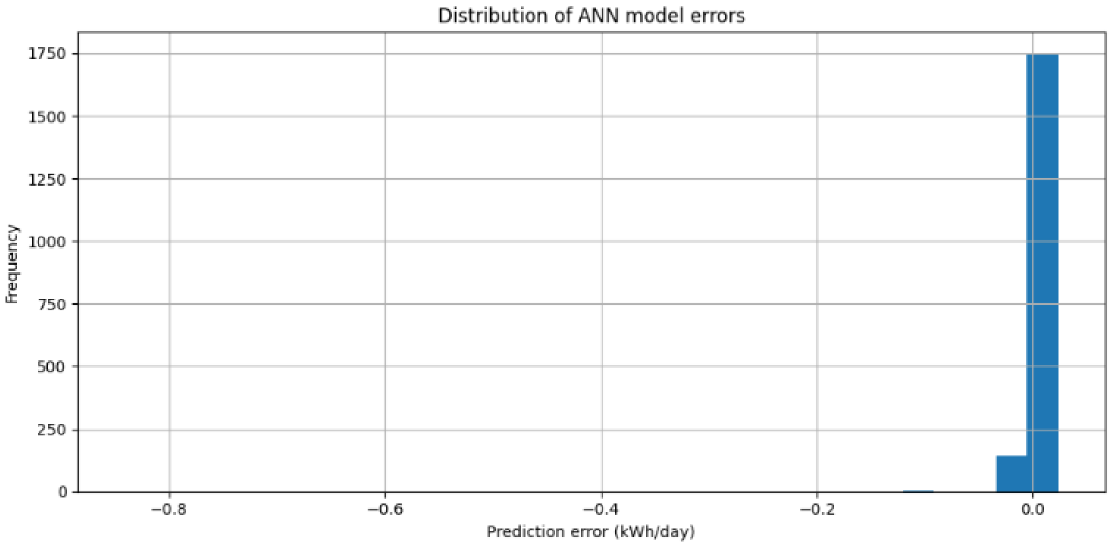

Figure 11. *Distribution of the prediction errors of the ANN model for the testing dataset.*

As shown in Figure 12, the learning curves exhibit a sharp drop in both training and validation losses during the initial epochs, followed by a steady convergence to very low values. The close match between the two curves throughout training suggests minimal overfitting and strong generalization of the ANN. This rapid and stable convergence further supports the effectiveness of the chosen 4–32–16–8–1 architecture and the Adam optimizer for reproducing the estimated photovoltaic potential.

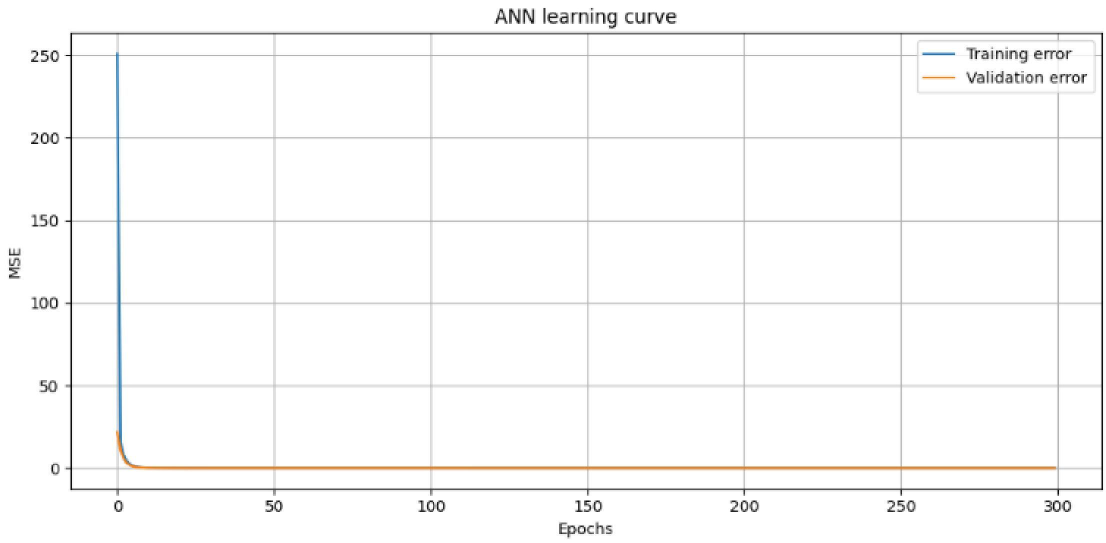

Figure 12. *Training and validation loss curves of the developed ANN model.*

Taken together, the results indicate that the ANN developed here is a dependable and accurate approach for modeling photovoltaic potential in Kankan. The very low prediction errors, together with the close correspondence between the estimated values and the ANN outputs, confirm the adequacy of the proposed method. These outcomes are consistent with the work of Mellit and Kalogirou [29], who demonstrated that artificial neural networks are among the most effective methods for modeling and predicting the performance of photovoltaic systems under complex climatic conditions.

3.4. Synthesis of the Climatic Effects on Photovoltaic Potential

To better gauge how pronounced the observed climatic changes are across the study periods, Figure 13 reports the relative shifts in climate variables and photovoltaic potential for 2011–2020 and 2021–2025, with 2000–2010 serving as the baseline. According to Figure 13, relative humidity changed the most, rising by 14.45% in 2011–2020 and by 18.44% in

2021–2025. By contrast, both air temperature and wind speed showed gradual declines, while global solar irradiation stayed essentially unchanged, with fluctuations under 0.3%. In line with this stability, the photovoltaic potential fell only slightly, by 0.38% and 1.00% relative to the reference period. This near-constancy in photovoltaic potential is largely due to the very small variation in global solar irradiation, which remains the main determinant of photovoltaic output. Recent studies also indicate that solar resources are relatively robust to climate change when irradiation changes are limited [19, 35, 46, 47]. The results for Kankan are consistent with this evidence and show that the observed shifts in air temperature, relative humidity, and wind speed did not produce a marked decrease in photovoltaic potential [21]. In addition, the combined effects of the climatic variables are not uniformly aligned. Lower air temperatures can enhance module efficiency by reducing thermal losses, whereas higher relative humidity tends to reduce performance. This partial offset between variables helps explain the modest change in photovoltaic potential and underscores the value of an integrated perspective when evaluating climate impacts on photovoltaic systems [47]. The strong performance of the artificial neural network in this study further shows that AI-based methods are suitable for modeling the complex links between climatic variables and photovoltaic potential. The ability of the developed ANN to reproduce the estimated photovoltaic potential with high accuracy highlights its usefulness for assessing and forecasting solar energy resources in tropical contexts [48]. Overall, the findings indicate that the climatic changes observed in Kankan between 2000 and 2025 have had only a limited effect on photovoltaic potential. This resilience of the solar resource is an advantage for the long-term rollout of photovoltaic energy in Guinea and, more broadly, in West Africa, where the energy transition increasingly depends on the sustainable use of renewable resources [49].

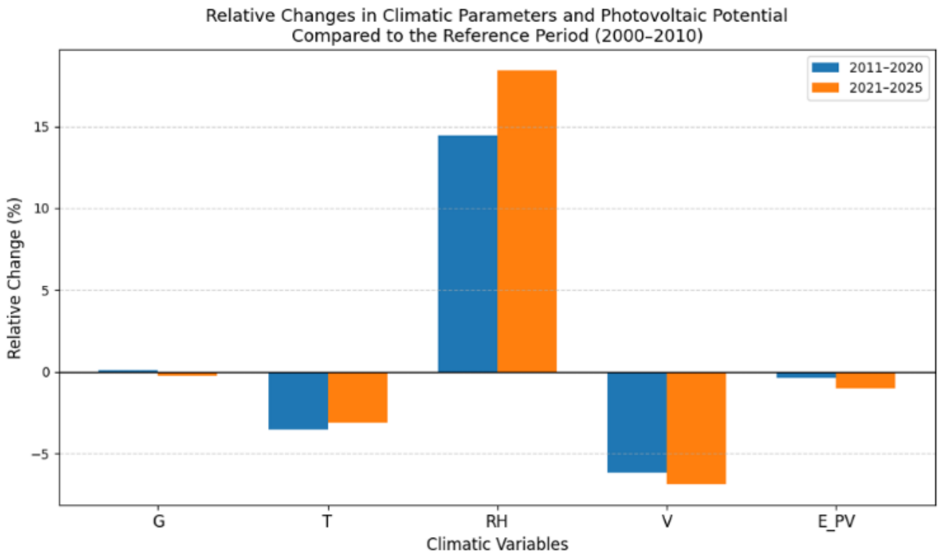

Figure 13. *Relative variations of climatic variables and photovoltaic potential with respect to the reference period (2000–2010).*

4. Conclusion

This work examined how climate variability affects the photovoltaic potential of Kankan, Guinea, using daily records from the NASA POWER database spanning 2000 to 2025. We identified marked trends in air temperature, relative humidity, and wind speed, while global solar irradiation showed little change. Despite these shifts, the estimated photovoltaic potential did not exhibit a significant trend, indicating that Kankan's solar resource has remained suitable for photovoltaic development over the past twenty-six years. An artificial neural network (ANN) built for this study reproduced the estimated photovoltaic potential with high accuracy using the climatic variables as inputs. Together, these results highlight the value of approaches based on artificial intelligence for analyzing and modeling renewable energy resources in tropical contexts. Several limitations should be acknowledged. The analyses relied on satellite-derived climate data from NASA POWER and a semi-empirical model to estimate photovoltaic potential. In addition, the ANN was trained on potential values generated by this semi-empirical model rather than on real photovoltaic production data. Even so, the approach provides an initial quantitative appraisal of how climate variability influences photovoltaic potential in Kankan. Future work should integrate measurements from local photovoltaic installations and climate projections from CMIP6 scenarios to evaluate the long-term evolution of the region's photovoltaic potential under future climate conditions. Such efforts would help strengthen sustainable energy planning in Guinea and, more broadly, across West Africa.

Abbreviations

AI	Artificial Intelligence
MPANN	Multilayer Perceptron Artificial Neural Network
GHI	Global Horizontal Irradiation
MAE	Mean Absolute Error
MAPE	Mean Absolute Percentage Error
MSE	Mean Squared Error
NASA POWER	National Aeronautics and Space Administration – Prediction Of Worldwide Energy Resources
NOCT	Nominal Operating Cell Temperature
PV	Photovoltaic
RMSE	Root Mean Squared Error
STC	Standard Test Conditions

Acknowledgments

The authors express their gratitude to the NASA Langley Research Center for providing access to the NASA POWER climate database used in this study.

Author Contributions

Papa Lat Tabara Sow: Conceptualization, Investigation, Methodology, Writing – original draft, Writing – review & editing

Mamadou Traore: Conceptualization, Data curation, Formal Analysis, Investigation, Methodology, Software, Validation, Visualization, Writing – original draft, Writing – review & editing

Daouda Gueye: Data curation, Formal Analysis, Software, Validation, Visualization

Amadou Sidibe: Investigation, Validation, Visualization, Writing – original draft, Writing – review & editing

Amadou Ba: Data curation, Formal Analysis, Software, Validation, Visualization

Cheikh Saliou Toure: Conceptualization, Investigation, Methodology, Software

Vone Beavogui: Writing – original draft, Writing – review & editing

Alphousseyni Ndiaye: Validation, Writing – original draft, Writing – review & editing

Senghane Mbodji: Supervision, Validation, Writing – original draft, Writing – review & editing

Faoro Eugene Maomou: Supervision, Validation, Writing – review & editing

Data Availability Statement

The NASA POWER climate data used in this research are publicly accessible at https://power.larc.nasa.gov/.

Conflicts of Interest

The authors state that they have no known financial conflicts of interest or personal relationships that could have influenced the work reported in this paper.

References

[1] K. Calvin et al., « IPCC, 2023: Climate Change 2023: Synthesis Report. Contribution of Working Groups I, II and III to the Sixth Assessment Report of the Intergovernmental Panel on Climate Change [Core Writing Team, H. Lee and J. Romero (eds.)]. IPCC, Geneva, Switzerland. », Intergovernmental Panel on Climate Change (IPCC), juill. 2023. https://doi.org/10.59327/IPCC/AR6-9789291691647

[2] L. Cozzi et T. Gould, « World Energy Outlook 2023 ». International Energy Agency, France. [En ligne]. Disponible sur: https://www.iea.org/reports/world-energy-outlook-2025

[3] D. Gielen, F. Boshell, D. Saygin, M. D. Bazilian, N. Wagner, et R. Gorini, « The role of renewable energy in the global energy transformation », Energy Strategy Rev., vol. 24, p. 38-50, avr. 2019, https://doi.org/10.1016/j.esr.2019.01.006

[4] « RENEWABLES 2023 GLOBAL STATUS REPORT ». [En ligne]. Disponible sur: https://www.ren21.net/wp-content/uploads/2019/05/GSR2023_GlobalOverview_Full_Report_with_endnotes_web.pdf

[5] « IRENA (2025), Renewable power generation costs in 2024, International Renewable Energy Agency, Abu Dhabi. » [En ligne]. Disponible sur: https://www.rinnovabili.it/wp-content/uploads/2025/07/IRENA-RENEWABLE-POWER-GENERATION-COSTS-IN-2024.pdf

[6] D. S. Philipps, F. Ise, W. Warmuth, et P. P. GmbH, « Photovoltaics Report », juin 2026, [En ligne]. Disponible sur: https://www.ise.fraunhofer.de/de/veroeffentlichungen/studien/photovoltaics-report.html

[7] T. Alex-Oke et al., « Renewable energy market in Africa: Opportunities, progress, challenges, and future prospects », Energy Strategy Rev., vol. 59, p. 101700, mai 2025, https://doi.org/10.1016/j.esr.2025.101700

[8] P. A. Owusu et S. Asumadu-Sarkodie, « A review of renewable energy sources, sustainability issues and climate change mitigation », Cogent Eng., vol. 3, no 1, p. 1167990, dec. 2016, https://doi.org/10.1080/23311916.2016.1167990

[9] E. Skoplaki et J. A. Palyvos, « On the temperature dependence of photovoltaic module electrical performance: A review of efficiency/power correlations », Sol. Energy, vol. 83, no 5, p. 614-624, mai 2009, https://doi.org/10.1016/j.solener.2008.10.008

[10] D. S. Hasan, Mansour S. Farhan, et H. Alrikabi, « Impact of Cloud, Rain, Humidity, and Wind Velocity on PV Panel Performance », Wasit J. Eng. Sci., vol. 10, no 2, p. 34-43, juin 2022, https://doi.org/10.31185/ejuow.Vol10.Iss2.237

[11] H. A. Kazem, S. Al-Bahri, S. Al-Badi, H. Al-Mahkladi, et A. H. A. Al-Waeli, « Dust Effect on the Performance of Photovoltaic », Adv. Mater. Res., vol. 875-877, p. 1908-1911, fevr. 2014, https://doi.org/10.4028/www.scientific.net/AMR.875-877.1908

[12] M. Erdenebat et S. Khayankhyarvaa, « Influence of Climatic Factors Affecting Photovoltaic System », vol. 10, no 6, 2023.

[13] S. Jerez et al., « The impact of climate change on photovoltaic power generation in Europe », Nat. Commun., vol. 6, no 1, p. 10014, dec. 2015, https://doi.org/10.1038/ncomms10014

[14] M. Wild, D. Folini, F. Henschel, N. Fischer, et B. Müller, « Projections of long-term changes in solar radiation based on CMIP5 climate models and their influence on energy yields of photovoltaic systems », Sol. Energy, vol. 116, p. 12-24, juin 2015, https://doi.org/10.1016/j.solener.2015.03.039

[15] C. Nichols, M. Hill, et X. Liu, « Climate Change Impacts on Solar Energy Generation in the Continental United States, Forecasts from Deep Learning », 2024, SSRN. https://doi.org/10.2139/ssrn.5044190

[16] T. AlSkaif, « A systematic analysis of meteorological variables for PV output power estimation », Renew. Energy, vol. 153, no 12-22, 2020, https://doi.org/10.1016/j.renene.2020.01.150

[17] P. Sarmah et al., « Comprehensive Analysis of Solar Panel Performance and Correlations with Meteorological Parameters », ACS Omega, vol. 8, no 50, p. 47897-47904, dec. 2023, https://doi.org/10.1021/acsomega.3c06442

[18] A. Bichet, B. Hingray, G. Evin, A. Diedhiou, C. M. F. Kebe, et S. Anquetin, « Potential impact of climate change on solar resource in Africa for photovoltaic energy: analyses from CORDEX-AFRICA climate experiments », Environ. Res. Lett., vol. 14, no 12, p. 124039, dec. 2019, https://doi.org/10.1088/1748-9326/ab500a

[19] D. K. Danso et al., « A CMIP6 assessment of the potential climate change impacts on solar photovoltaic energy and its atmospheric drivers in West Africa », Environ. Res. Lett., vol. 17, no 4, p. 044016, avr. 2022, https://doi.org/10.1088/1748-9326/ac5a67

[20] M. Agbor et al., « Effects of Angstrom-Prescott and Hargreaves-Samani Coefficients on Climate Forcing and Solar PV Technology Selection in West Africa », Trends Renew. Energy, vol. 9, no 1, p. 78-106, mars 2023, https://doi.org/10.17737/tre.2023.9.1.00150

[21] Y. E. Alami et al., « Numerical exploration and relational impact ranking of critical parameters in 3D PV module studies », Results Eng., vol. 27, p. 107097, sept. 2025, https://doi.org/10.1016/j.rineng.2025.107097

[22] E. H. Honningdalsnes, E. S. Marstein, M. M. Nygård, M. S. Wiig, et H. N. Riise, « Benchmarking irradiation models for photovoltaic applications: A comparative analysis of radiance-based tools », Sol. Energy, vol. 296, p. 113566, août 2025, https://doi.org/10.1016/j.solener.2025.113566

[23] M. Yang, H. Zhang, X. Yu, A. S. Seklouli, A. Bouras, et Y. Ouzrout, « A composite photovoltaic power prediction optimization model based on nonlinear meteorological factors analysis and hybrid deep learning framework », Int. J. Electr. Power Energy Syst., vol. 169, p. 110660, août 2025, https://doi.org/10.1016/j.ijepes.2025.110660

[24] M. Agoundedemba, C. K. Kim, et H.-G. Kim, « Energy Status in Africa: Challenges, Progress and Sustainable Pathways », Energies, vol. 16, no 23, p. 7708, nov. 2023, https://doi.org/10.3390/en16237708

[25] « Pays : Republique de Guinee Evaluation et Analyse des Gaps par rapport aux objectifs de SE4ALL ». [En ligne]. Disponible sur: https://www.se4all-africa.org/fileadmin/uploads/se4all/Documents/Country_RAGAs/Guinea_RAGA_FR_Released.pdf

[26] N. Diaby, M. A. Camara, S. Soumah, et A. Sakouvogui, « Experimental Assessment of Solar Irradiance in Kankan and Validation of a Photovoltaic Resource Prediction Model », Open J. Appl. Sci., vol. 16, no 05, p. 1793-1811, 2026, https://doi.org/10.4236/ojapps.2026.165099

[27] « NASA. (2023). NASA POWER Data Access Viewer. NASA Langley Research Center. » Consulte le: 16 juin 2026. [En ligne]. Disponible sur: https://power.larc.nasa.gov/data-access-viewer/

[28] V. A. Jimenez, A. Barrionuevo, A. Will, et S. Rodríguez, « Neural Network for Estimating Daily Global Solar Radiation Using Temperature, Humidity and Pressure as Unique Climatic Input Variables », Smart Grid Renew. Energy, vol. 07, no 03, p. 94-103, 2016, https://doi.org/10.4236/sgre.2016.73006

[29] A. Mellit et S. A. Kalogirou, « Artificial intelligence techniques for photovoltaic applications: A review », Prog. Energy Combust. Sci., vol. 34, no 5, p. 574-632, oct. 2008, https://doi.org/10.1016/j.pecs.2008.01.001

[30] N. Premalatha et A. Valan Arasu, « Prediction of solar radiation for solar systems by using ANN models with different back propagation algorithms », J. Appl. Res. Technol., vol. 14, no 3, p. 206-214, juin 2016, https://doi.org/10.1016/j.jart.2016.05.001

[31] J. A. Duffie et W. A. Beckman, Solar Engineering of Thermal Processes, 1re ed. Wiley, 2013. https://doi.org/10.1002/9781118671603

[32] H. B. Mann, « Nonparametric Tests Against Trend », Econometrica, vol. 13, no 3, p. 245, juill. 1945, https://doi.org/10.2307/1907187

[33] B. Y. Menna et D. K. Waktola, « Extreme temperature trend and return period mapping in a changing climate in Upper Tekeze river basin, Northern Ethiopia », Phys. Chem. Earth Parts ABC, vol. 128, p. 103234, dec. 2022, https://doi.org/10.1016/j.pce.2022.103234

[34] I. Dabanli, E. Şişman, Y. S. Güçlü, M. E. Birpınar, et Z. Şen, « Climate change impacts on sea surface temperature (SST) trend around Turkey seashores », Acta Geophys., vol. 69, no 1, p. 295-305, fevr. 2021, https://doi.org/10.1007/s11600-021-00544-2

[35] Y. J. Then et S. Abdul Halim, « Modified Mann-Kendall with higher-order statistics for trend analysis », Sci. Rep., vol. 16, no 1, p. 500, dec. 2025, https://doi.org/10.1038/s41598-025-30034-0

[36] E. Aksay, E. Çoban, et Y. S. Güçlü, « Normalized innovative trend analysis model and Mann-Kendall test for solar data », Model. Earth Syst. Environ., vol. 11, no 5, p. 347, oct. 2025, https://doi.org/10.1007/s40808-025-02550-5

[37] C. Banes et al., « Developpement d'un modèle semi-analytique pour la prediction du comportement thermique et energetique d'un panneau photovoltaïque en conditions reelles de fonctionnement », 2024, https://doi.org/10.25855/SFT2024-017

[38] T. Chai et R. R. Draxler, « Root mean square error (RMSE) or mean absolute error (MAE)? – Arguments against avoiding RMSE in the literature », Geosci. Model Dev., vol. 7, no 3, p. 1247-1250, juin 2014, https://doi.org/10.5194/gmd-7-1247-2014

[39] H. Verbois, Y.-M. Saint-Drenan, A. Thiery, et P. Blanc, « Statistical learning for NWP post-processing: A benchmark for solar irradiance forecasting », Sol. Energy, vol. 238, p. 132-149, mai 2022, https://doi.org/10.1016/j.solener.2022.03.017

[40] T. Laepple et al., « Regional but not global temperature variability underestimated by climate models at supradecadal timescales », Nat. Geosci., vol. 16, no 11, p. 958-966, nov. 2023, https://doi.org/10.1038/s41561-023-01299-9

[41] C. Deser, A. Phillips, V. Bourdette, et H. Teng, « Uncertainty in climate change projections: the role of internal variability », Clim. Dyn., vol. 38, no 3-4, p. 527-546, fevr. 2012, https://doi.org/10.1007/s00382-010-0977-x

[42] Intergovernmental Panel On Climate Change, Ed., « Climate Phenomena and their Relevance for Future Regional Climate Change », in Climate Change 2013 – The Physical Science Basis, 1re ed., Cambridge University Press, 2014, p. 1217-1308. https://doi.org/10.1017/CBO9781107415324.028

[43] D. Ospina et al., « Ten New Insights in Climate Science 2025 », https://doi.org/10.1017/sus.2025.10043

[44] P. M. M. Soares, M. C. Brito, et J. A. M. Careto, « Persistence of the high solar potential in Africa in a changing climate », Environ. Res. Lett., vol. 14, no 12, p. 124036, dec. 2019, https://doi.org/10.1088/1748-9326/ab51a1

[45] D. Faiman, « Assessing the outdoor operating temperature of photovoltaic modules », Prog. Photovolt. Res. Appl., vol. 16, no 4, p. 307-315, juin 2008, https://doi.org/10.1002/pip.813

[46] P. Adigun, K. Dairaku, A. T. Ogunrinde, et X. Xue, « Climate-driven synchronization of solar extremes threatens the resilience of Africa's regional power pool », Npj Clean Energy, vol. 2, no 1, p. 11, mai 2026, https://doi.org/10.1038/s44406-026-00027-7

[47] S. Obahoundje et al., « Teal-WCA: A Climate Services Platform for Planning Solar Photovoltaic and Wind Energy Resources in West and Central Africa in the Context of Climate Change », Data, vol. 9, no 12, p. 148, dec. 2024, https://doi.org/10.3390/data9120148

[48] R. Asghar, F. R. Fulginei, M. Quercio, et A. Mahrouch, « Artificial Neural Networks for Photovoltaic Power Forecasting: A Review of Five Promising Models », IEEE Access, vol. 12, p. 90461-90485, 2024, https://doi.org/10.1109/ACCESS.2024.3420693

[49] T. I. Ingo, L. Gyoh, Y. Sheng, M. K. Kaymak, A. D. Şahin, et H. M. Pouran, « Accelerating the Low-Carbon Energy Transition in Sub-Saharan Africa through Floating Photovoltaic Solar Farms », Atmosphere, vol. 15, no 6, p. 653, mai 2024, https://doi.org/10.3390/atmos15060653